MDPI

Article

An Experimental Investigation of the Flexural Strength and Fracture Toughness of Granular Snow Ice Under a Three-Point Bending Test

Hongwei Han [1,2], Wanyun Li [1], Yu Li [1,*] , Zhi Liu [1] and Xingchao Liu [1,*]

[1] School of Water Conservancy and Civil Engineering, Northeast Agricultural University, Harbin 150030, China; hanhongwei@neau.edu.cn (H.H.); 18845147160@163.com (W.L.); 17853819179@163.com (Z.L.)
[2] Heilongjiang Provincial Key Laboratory of Water Resources and Water Conservancy Engineering in Cold Region, Northeast Agricultural University, Harbin 150030, China
* Correspondence: 18846771809@163.com (Y.L.); dnlxc@neau.edu.cn (X.L.)

Abstract: Ice is a common natural phenomenon in cold areas, which plays an important role in the construction of cold areas and the design of artificial ice rinks. To supplement our knowledge of ice mechanics, this paper investigates the mechanical properties of granular snow ice. The factors influencing the flexural strength of granular snow ice are analyzed through a three-point bending test. It is found that flexural strength is affected by strain rate. At low strain rates, flexural strength increases with increasing strain rate, whereas at high strain rates, flexural strength decreases with increasing strain rate. As temperature decreases, the flexural strength value of ice increases, but its brittleness becomes more pronounced, indicating that the strain rate corresponding to the maximum flexural strength is lower. Within the test temperature range, the tough-brittle transition range is from $6.67 \times 10^{-5} \text{ s}^{-1}$ to $3.11 \times 10^{-4} \text{ s}^{-1}$. At $-5\,^\circ\text{C}$, the strain rate corresponding to the maximum bending strength is $3.11 \times 10^{-4} \text{ s}^{-1}$, while at $-10\,^\circ\text{C}$, it is only $6.67 \times 10^{-5} \text{ s}^{-1}$. Flexural strength is influenced by crystal structure. At $-20\,^\circ\text{C}$, the average flexural strength of granular snow ice is 2.85 MPa, compared to 1.93 MPa for columnar ice at the same temperature. Through observation, we found that there are straight cracks and oblique cracks. The fracture toughness of granular snow ice was investigated by cutting prefabricated cracks at the bottom of the ice beam and employing a three-point bending device. It is found that fracture toughness decreases with increasing strain rate. Temperature also affects granular snow ice. At $-15\,^\circ\text{C}$, fracture toughness is $181.60 \text{ kPa} \cdot \text{m}^{1/2}$, but at $-6\,^\circ\text{C}$, it decreases to $147.28 \text{ kPa} \cdot \text{m}^{1/2}$. However, at varying temperatures and strain rates, there is no significant difference in the fracture patterns of ice samples, which predominantly develop upward along the prefabricated cracks.

Keywords: granular snow ice; ice temperature; strain rate; flexural strength; fracture toughness

1. Introduction

Ice is a non-homogeneous composite material consisting of grains, grain boundaries, and initial defects [1,2], with types including sea ice, river ice, lake ice, reservoir ice, icebergs, permafrost, atmospheric ice, and polar glaciers in cold regions [3]. Ice, as a widespread natural phenomenon in cold regions, has beneficial aspects for human life, such as enabling the development of oil resources in the polar seas [4]. Moreover, ice itself serves as a load-bearing platform, capable of supporting and transporting both mobile and stationary heavy loads [5]. Ice on rivers and lakes has long been utilized for ice tourism, recreation, and ice transportation [6]. However, ice-related disasters, including river ice floods, reservoir ice impacts on gates, slope protection, and winter operations of power plants, as well as the effects of sea ice on offshore structures and navigation, pose significant threats to life and property [7]. In the design, construction, and operation of hydroelectric equipment, as well as in the design of structures such as icebreakers, special consideration must be

given to ice loads to ensure operational safety in cold regions [8,9]. When ice interacts with inclined or conical structures, bending failure typically occurs [10]. It is not only an important mechanical property for assessing the climbing and impact strength of ice on inclined hydraulic structures [11], but also a key parameter for calculating ice loads [8]. Ice fracture destruction is also common. It is an important parameter in the design of hydraulic structures and the analysis of river ice dynamics. Following the formation of the ice layer, the force generated by its heating and expansion is the primary load that leads to the failure of reservoir slope protection [12]. Extreme ice pressure is related to the deformation and fracture behavior of the ice sheet under compression. To develop an extreme ice pressure model based on fracture mechanics theory, it is particularly necessary to understand the fracture toughness of ice [13].

In 1968, Weeks and Assur demonstrated that sea ice exhibits viscoelastic mechanical properties [14]. Sinha [15] argued that the viscoelastic–plastic constitutive relationship of sea ice allows it to exhibit a wide range of mechanical behaviors at different loading rates. Previous research has found that ice shows brittleness at higher strain rates, while lower rates lead to ductile behavior [16–19]. Specifically, the low-strain-rate region exhibits ductile failure, the high-strain-rate region is characterized by brittle failure, and there is a ductile-to-brittle transition stage in between. Zhang et al. [20] discovered that the transition range for ice from ductile to brittle is between 1.46×10^{-6} s^{-1} and 3.54×10^{-5} s^{-1} on freshwater ice. Schulson [21,22] first proposed the critical grain size of ice in analyzing the transition from brittle to ductile behavior, concluding that this transition in the properties of ice materials is related to grain size. Additionally, many scholars use theoretical or experimental methods to describe the transition of ice from exhibiting ductile behavior to brittle behavior [23,24].

Currently, experimental studies on ice bending mainly include three-point bending, four-point bending, and cantilever beam tests. Of these, three-point bending tests involve retrieving ice samples and preparing them indoors, while cantilever beam tests are predominantly conducted in the field [25]. In 1943, the Brazilian engineer Carneiro [26] proposed the famous Brazilian disk indirect tensile test method, which is now widely used to test the tensile strength of rocks, concrete, and other brittle materials [27]. There are a number of methods to test brittle materials for mixed-mode (I + II) or pure-mode II fracture toughness, such as using straight-notched Brazilian disks, V-notched Brazilian disks, and compression short-core tests [28–30]. Xiao et al. [31] concluded that under the premise of ensuring that ice is a brittle material, it can be tested as a rock and the fracture toughness and tensile strength can be measured by applying Brazilian disk splitting.

The mechanical properties of ice may depend on a combination of factors, such as crystal structure, temperature, porosity, grain size, and strain rate [32,33]. In general, the fracture toughness of ice is in the range of 50–150 kPa·m$^{1/2}$ [34], increasing slightly with decreasing temperature [35] and decreasing with increasing grain size [36] and porosity [37]. Wang [38] conducted a three-point bending test on artificial columnar ice and found that the flexural strength increased and then decreased with an increase in the strain rate, and a fitting relationship between flexural strength, elastic modulus, and strain rate was obtained. Gagnon [39] and Ji et al. [40] conducted bending tests on glacier ice and sea ice, respectively, and found that the flexural strength increased with an increase in strain rate and a decrease in temperature. Zhang et al. [41] studied freshwater granular ice and found that the flexural strength initially decreases, then increases, and then decreases again with increasing stress rate. Zhang [42] found that the variation in flexural strength with strain rate is similar to an inverted "W" shape. Xu et al. [43] conducted three-point bending tests with notches on pure polycrystalline ice at different temperatures (−20 °C, −30 °C, and −40 °C) and loading rates (1 to 100 mm/min). They found that when the strain rate at the crack tip was less than the critical value of 6×10^{-3} s^{-1}, the fracture toughness decreased with the increasing crack tip strain rate. Beyond this critical value, the fracture toughness remained constant. Litwin et al. [44] studied the tensile strength and fracture toughness within the temperature range of 260 K to 110 K and found that fracture toughness is not sensitive to

temperature. Mulmule et al. [45] and Dempsey et al. [46] conducted fracture toughness tests on sea ice of different sizes and found a significant size effect. Dempsey et al. [46] suggested that the results of fracture tests can be characterized by tensile strength, which decreases with increasing specimen size.

Ice plays a role in transportation, the military, and other fields, and has also led to the development of numerous ice sports [47]. Some countries use refrigeration technology to manufacture artificial ice rinks, in which the artificial ice surfaces must meet the requirements of stiffness and bearing capacity, as well as ensure the normal requirements of ice sports. However, when moving on the ice surface, it may crack or be locally damaged, causing harm. Therefore, investigating the mechanical properties of artificial ice is essential. Due to variations in growth environments, different types of ice crystals form, including snow ice, granular ice, and columnar ice [48]. However, previous studies have provided relatively little research on the mechanics of granular ice. In field experiments, the relatively low content of granular ice and uneven thickness in the ice layer sometimes hinder the extraction of a sufficient number of samples, making it difficult to stably test its mechanical properties. Studies [8] also indicate that the bending strength of granular ice is higher than that of columnar ice, necessitating a serious consideration of its mechanical properties. Schwarz et al. [49] provided recommendations for the dimensions of ice specimens in bending tests. The focus of this study is to prepare artificial granular ice in the laboratory, cut a small ice sample measuring 35 mm × 35 mm × 180 mm, and investigate the influence of temperature and strain rate on the bending strength and fracture toughness of granular ice through three-point bending and fracture toughness tests, aiming to further supplement the mechanical properties of ice.

2. Method

2.1. Ice Sample Preparation

As a result of changes in climate and temperature, the three states of water are constantly shifting. As temperatures continue to drop to freezing point, bodies of water develop ice. During crystallization, water forms different crystal structures due to various external conditions such as temperature and pressure, and crystals with the same structure are affected by the environment, resulting in different grain sizes [32]. In rivers, for example, granular snow ice crystals may form during the early stages of freezing when the ice grows too fast or when snow falls before cooling, after which the vertical growth rate dominates and columnar ice crystals are formed [50].

The granular ice and columnar ice samples used in this study were prepared at Northeast Agricultural University in Harbin, Heilongjiang Province, China. The specific steps for the preparation of granular ice are as follows: add about one-third of tap water into a container wrapped with foam board, place it in a sub-zero environment and cool it down to 0 °C, then add slush and stir it to form an ice–water mixture, and finally invert the container to remove the ice after it is completely frozen. Columnar ice was prepared in the low-temperature laboratory, with a temperature control range of room temperature to −40 °C and a temperature fluctuation value of ±0.5 °C. Due to the addition of snow mud during the preparation process to form an ice–water mixture, we will use "granular snow ice" to describe the experimental object in the following description.

Cracks and large fractures in the middle of the ice body significantly impact test results, so any specimen exhibiting these conditions should be promptly discarded [2]. To prevent weathering and adhesion, the specimens were wrapped in cling film and transported in a foam box. The entire process of ice mechanics testing requires temperature control. Temperature control includes sample storage, keeping a constant temperature, and loading processes. After sample preparation is complete, the ice sample should be stored in a −15 °C freezer to ensure the long-term preservation and stability of the ice crystal structure. Before starting the experiment, the time required for the ice sample to reach thermal equilibrium should be calculated using the heat conduction equation, based on the sample size and temperature difference. Then, place the ice sample in the freezer for a

duration exceeding the calculated time to ensure thermal equilibrium. After 48 h, the ice sample will achieve full thermal equilibrium [50].

2.2. Ice Crystal Structure Measurement

In general, the internal organization of ice reflects its growth history and determines its fundamental physical properties; thus, observing the structural characteristics of ice's internal organization is an essential task. Based on prior research [32], ice flakes were prepared in a low-temperature laboratory and observed using a Rigsby universal stage. The Rigsby universal stage employs a polarizing microscope to measure the spatial orientation of linear and planar elements within the flakes, enabling the direct visualization of the particle size and shape of the observed samples. The specific steps include the following: Select a vertical and intact ice sample, and use a planer to flatten the protruding defects on the observed surface. Secondly, place the ice sample in contact with a glass sheet at a temperature slightly above 0 °C, moving the sample left and right on the glass to expel air bubbles. And then, freeze the glass sheet with the ice sample at a low temperature, then use a planer to thin the ice sample to about a 1 mm thickness after it is solidly frozen, and mark it clearly. To avoid weathering, place the completed ice slices in a sealed plastic bag and store them at a low temperature and then observe the ice slices in a dark room using a Rigsby universal stage.

2.3. Three-Point Bending Test

2.3.1. Test Devices

This test uses the WDW-100 electronic universal testing machine, with a maximum test force of 100 kN, displacement measurement resolution of 0.01 mm, and a loading rate range of 0.005 to 1000 mm/min. It comes from Changchun Kexin Testing Instrument Co., Ltd. located in Changchun city, China. The test machine can perform tensile, bending, shear, and other tests in conventional and low-temperature environments [49]. In order to maintain a low temperature environment during the test, a low-temperature test chamber with a temperature accuracy of ± 1 °C is used [38]. Additionally, to adjust the distance between the specimen and the indenter and effectively observe the fracture pattern of the specimen during the loading process, etc., the lighting switch can be turned on. Figure 1 shows the WDW-100 electronic universal testing machine and the testing zone.

(a)

(b)
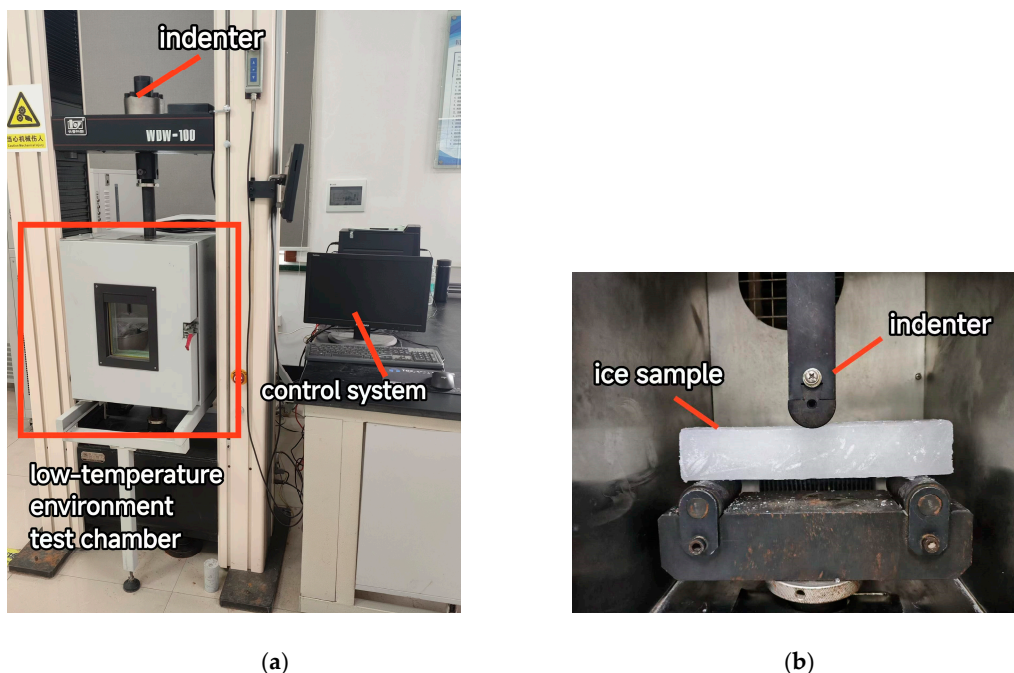
Figure 1. Test devices. (**a**) WDW–100 electronic universal testing machine. (**b**) Testing zone.

2.3.2. Test Principles and Procedures

Ice exhibits viscoelastic properties and is not entirely elastic. Gold demonstrated that between $-40\,°C$ and $-3\,°C$, ice approximates to a purely elastic material, permitting the application of elastic theory to analyze its failure and determine effective flexural strength values [51].

Ice is a viscoelastic plastic material. Han et al. [32] utilized linear elasticity theory to estimate the bending strength of columnar granular freshwater ice subjected to three-point bending beam tests. This study also fulfills the application conditions of linear elasticity theory, that is, takes place under the action of midspan loads, whereby the bending strength formula for a rectangular cross-section of a linear elastic, uniformly simply supported beam is as follows:

$$\sigma_f = \frac{3PL}{2bh^2} \tag{1}$$

where P is the load at which a three-point simply supported beam fails, b is the width of the beam, h is the height of the beam, and L is the span of the ice beam which is 150 mm.

Due to the existence of dimensional differences between the specimens, the specimen size data need to be measured again before each test, and the displacement loading rate is converted into the strain rate to unify the independent variable. According to the method proposed by Han et al. [32], the strain and strain rate at the bottom of the span of an ice beam are estimated according to the relationship between the strain and the deflection of a three-point simply supported beam:

$$\varepsilon = \frac{6h\delta}{L^2} \tag{2}$$

$$\dot{\varepsilon} = \frac{6h\dot{\delta}}{L^2} \tag{3}$$

where ε is the strain at the load application point, $\dot{\varepsilon}$ is the strain rate at the bottom of the load application point, δ is the deflection, which refers to the displacement of the point of action, and $\dot{\delta}$ is the displacement loading rate. When the ice sample fractures during the bending test, the test is immediately terminated and data are recorded.

Before the test, adjust the temperature of the environmental test chamber. and pre-cool for 30 min. Before the experiment, observe whether there are bubbles, impurities, and cracks in the sample and record them, and measure the size of the sample [38]. After everything is ready, place the specimen into the environmental test chamber on the fixed three-point bending fixture, aligning the indenter with the center of the specimen. And then, set the loading rate within the test machine program, number the specimen, and start loading. Before the sample is destroyed, the testing machine program continuously collects data and automatically saves the data information. After the experiment is completed, record the form of sample damage and clean the testing machine.

In this study, three-point bending tests of simply supported beams are performed on granular snow ice at $-5\,°C$, $-8\,°C$, $-10\,°C$, $-15\,°C$, $-18\,°C$, $-20\,°C$, $-25\,°C$, $-30\,°C$, and $-35\,°C$, for a total of nine working conditions, and on columnar ice at $-20\,°C$.

2.4. Fracture Toughness Test

2.4.1. Test Principles

According to fracture mechanics, crack growth occurs when the incremental energy available from the release of stored potential energy is equal to, or exceeds, that required to create new fracture surfaces. Resistance to crack growth is defined by fracture toughness, which is the amount of work required to propagate a crack by unit area [43]. Wei et al. [52] believe that fracture toughness K_{IC} is the stress intensity factor corresponding to unstable fracture of materials. In a three-point bending test, the specimen does not undergo simple stretching, and, thus, K_{IC} lacks an analytical solution. Concerning the measurement

of fracture toughness, there is no uniform standard, and various research results have a high degree of dispersion. Huang [53] calculated the fracture toughness of granular and columnar Yellow River ice. Based on the method given by Huang [53], the fracture toughness of granular ice was calculated in this paper:

$$K_{IC} = \frac{PL}{BW^{3/2}}P\left(\frac{a}{W}\right) \tag{4}$$

$$P\left(\frac{a}{W}\right) = 3(a/W)^{1/2} \times \frac{1.99 - (a/W)(1 - a/W)\left[2.15 - 3.93(a/W) + 2.70(a/W)^2\right]}{2(1 + 2a/W)(1 - a/W)^{3/2}} \tag{5}$$

where K_{IC} is the fracture toughness of the specimen, kPa·m$^{1/2}$.

2.4.2. Test Procedures

Unlike the bending test, the three-point bending fracture test requires pre-fabricated cracks to be machined in the center of the specimen to ensure that failure occurs at the loading point. The ratio of the length of the pre-fabricated crack to the height W of the specimen should be between 0.2 and 1 [2], while in this study, it is between 0.28 and 0.36. When using a saw bone machine for ice cutting, it is essential to ensure that the saw blade is perpendicular to the ice surface during processing and to apply even force throughout the process [2]. The loading method and structural dimensions of the specimens are shown in Figure 2.
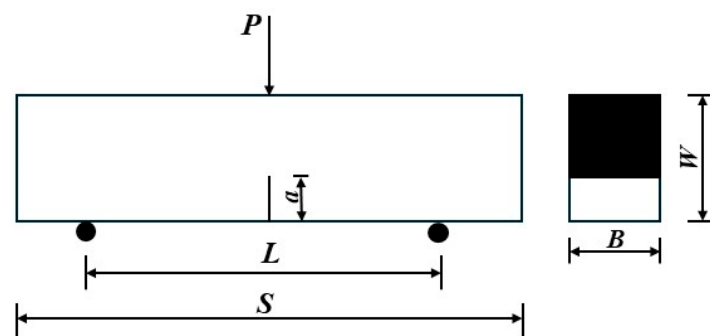
Figure 2. A schematic diagram of ice-sample loading (here, *L*, *S*, *W*, and *B* represent the ice beam's span, length, height, and thickness, respectively; a is the initial crack length, and *P* is the applied load).

The effects of temperature and loading rate on the ice beam were considered. Four temperatures were tested: −6 °C, −8 °C, −10 °C, and −15 °C. The displacement loading rates included eight types: 0.05 mm/min, 0.1 mm/min, 0.3 mm/min, 0.5 mm/min, 1 mm/min, 3 mm/min, 5 mm/min, and 10 mm/min.

For the preparation work before the experiment, refer to Section 2.3.2. After precooling is completed, remove the ice sample from the freezer. Prefabricated cracks may remain filled with foam or frost and should be cleaned with a planer to ensure they run through from top to bottom. Measure the width, height, and crack length of the ice sample and input these dimensions into the tester program.

3. Results and Analysis

3.1. Crystal Structure of Granular Snow Ice

Figure 3 shows a horizontal sheet of granular snow ice. As can be seen from the figure, the artificial ice prepared in the laboratory is a typical granular ice structure [32]. Slush is added in the icing process to form a mixture of ice water, and the growth rate of ice crystals is relatively high, resulting in the formation of granular ice crystals.
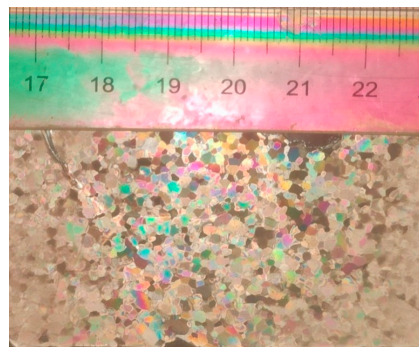
Figure 3. Horizontal slice of granular snow ice.

3.2. Three-Point Bending Test

3.2.1. Fracture Process Curve

Figure 4 presents a typical curve of flexural stress over time in a three-point bending test, which was conducted at −5 °C with a loading rate of 5 mm/min and a duration of 7.64 s. The ice beam undergoes three stages from loading to failure. At the beginning of loading, the load is small, the stress on the cross-section of the ice beam is also minimal, and microcracks produced at the edges of bubbles and impurities are negligible. The ice beam undergoes elastic deformation, with stress and strain maintaining a linear relationship; this is the first stage. As the load increases, because the tensile strength of ice is lower than its compressive strength, the tensile zone on the lower surface of the ice beam reaches its tensile strength, resulting in plastic deformation and crack formation, while the compressive zone remains in elastic deformation. This is the second stage. The load continues to increase until the strain at the lower surface of the ice beam exceeds the tensile limit strain, causing the original microcracks to develop into macrocracks. At this point, the ice near the neutral axis remains uncracked. With the increasing load, the cracks rapidly extend upward until the ice beam completely fractures. At this stage, the applied load exceeds the bending capacity of the ice, marking the third stage of ice beam failure [41].
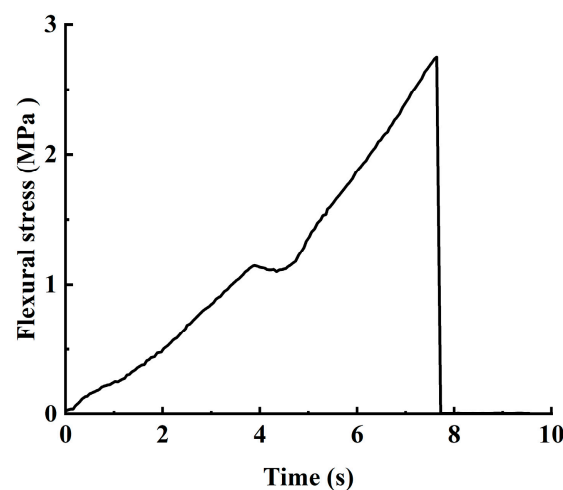

Figure 4. The curve of flexural stress over time in the three-point bending test.

Taking into account the uncontrollability of errors, four to six repeated tests were conducted for each loading rate and temperature, followed by the calculation of the average bending strength. The bending strength of granular snow ice ranged from 1.68 to 3.65 MPa, with an average of 2.89 ± 0.27 MPa; for columnar ice, it ranged from 1.50 to 2.36 MPa, averaging 1.69 MPa.

3.2.2. The Relationship Between Flexural Strength and Strain Rate

As shown in Figure 5, the relationship between the flexural strength of granular snow ice at different temperatures and loading rates is presented. The flexural properties of ice are influenced by the strain rate, showing a trend where flexural strength initially increases and then decreases with strain rate at each temperature. Previous research results have suggested that ice demonstrates toughness at low strain rates and brittleness at high strain rates [16–19]. Our results show that the ultimate flexural strength of ice occurs within the ductile–brittle transition interval, which ranges from 6.67×10^{-5} s^{-1} to 3.11×10^{-4} s^{-1} at the tested temperatures.
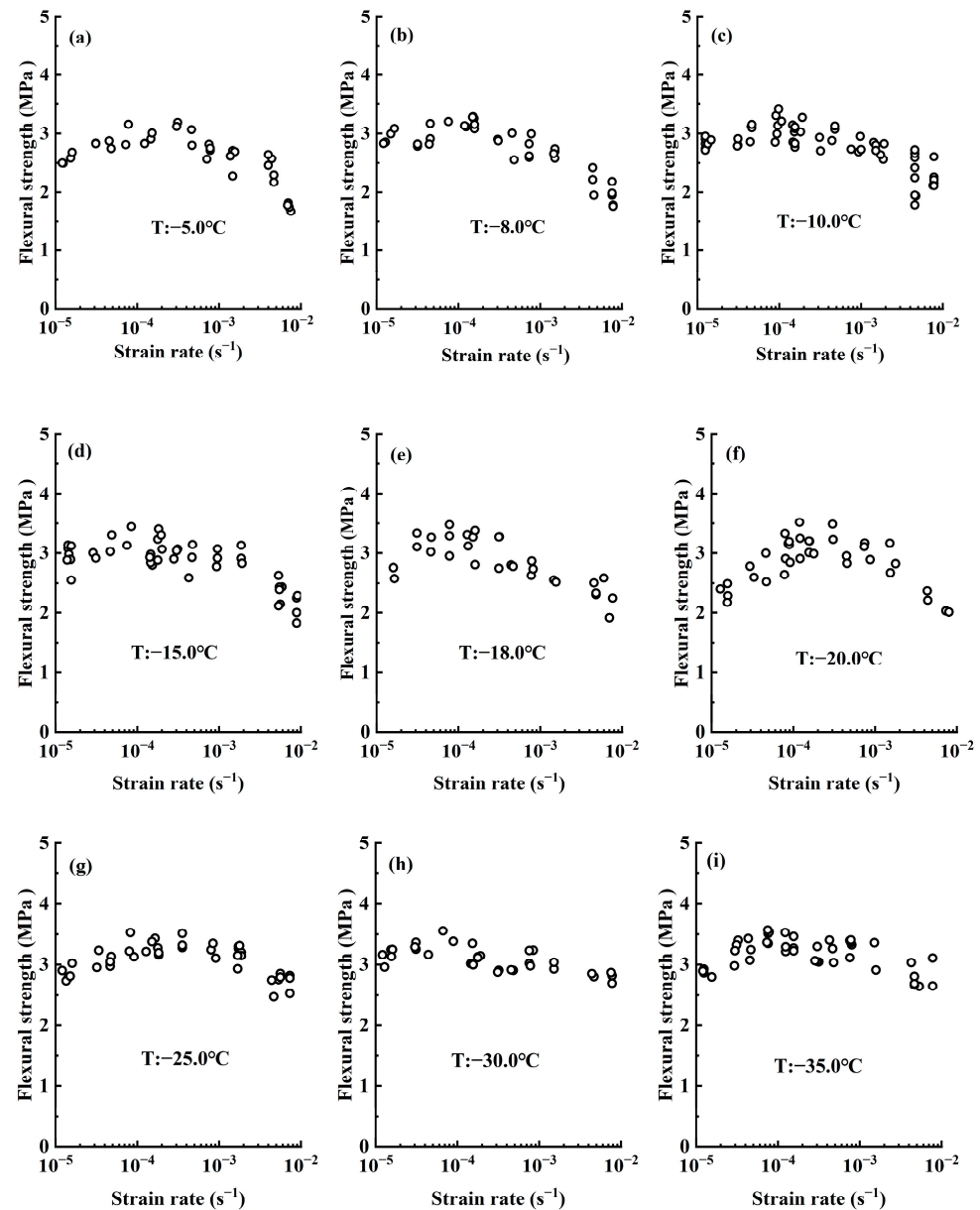
Figure 5. The flexural strength of granular snow ice at different temperatures and strain rates. (**a**–**i**) is the bending strength variation trend with strain rate at −5 °C, −8 °C, −10 °C, −15 °C, −18 °C, −20 °C, −25 °C and −30 °C and −35 °C, respectively.

Gagnon et al. [39] conducted bending tests on glacier ice at strain rates ranging from 10^{-5} s^{-1} to 10^{-3} s^{-1} and temperatures from $-16\,°C$ to $-1\,°C$. They found that at $-11\,°C$, the bending strength at a strain rate of 10^{-3} s^{-1} was approximately 26% higher than at 10^{-5} s^{-1}. The results of this paper align well with Gagnon's findings. For granular snow ice at $-5\,°C$, the average flexural strength at a strain rate of 10^{-3} s^{-1} is 17% higher than at 10^{-5} s^{-1}. And when the strain rate is less than 3.11×10^{-4} s^{-1}, the flexural strength of ice increases with the increase in strain rate, and the maximum value of flexural strength is 3.19 MPa. Above this strain rate, the flexural strength decreases with the increase in strain rate, and the minimum value of flexural strength is 1.68 MPa when the strain rate is 6.89×10^{-3} s^{-1}.

3.2.3. The Relationship Between Flexural Strength and Temperature

At $0\,°C$, the flexural strength of ice is close to 0 MPa, and the linear model cannot accurately predict the mechanical properties of ice at this temperature. Wang et al. [38] used logarithmic fitting to obtain the relationship between the bending strength and temperature of artificial ice:

$$\sigma_f = A + B\,ln(|T/T_0|) \tag{6}$$

in the formula, to coordinate units, the independent variable is adjusted to T/T_0, where T_0 is the temperature of $1\,°C$.

Temperature affects the mechanical properties of ice. In this experiment, three-point bending tests were conducted on granular snow ice from $-35\,°C$ to $-5\,°C$. Figure 6 shows the logarithmic fitting effect between the average flexural strength and ice temperature. It was found that the flexural strength increased as the temperature decreased. This occurs because lower ice temperatures increase the intermolecular linkage force, requiring more energy to produce cracks, thereby increasing ice strength and flexural strength.
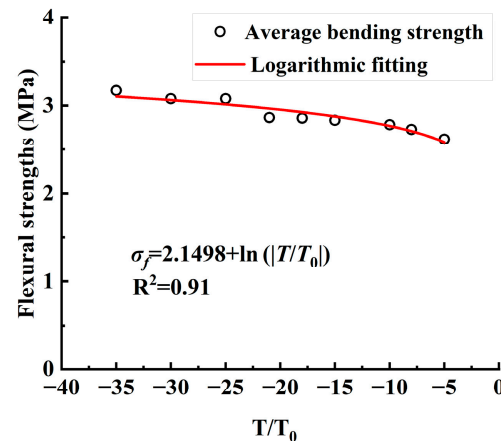
Figure 6. Logarithmic simulation of average flexural strength and ice temperature of granular snow ice.

Han et al. [54] concluded that the lower the temperature of the ice beam, the more pronounced the brittleness characteristics, which is manifested by the lower strain rate corresponding to the maximum ultimate flexural strength. The ductile–brittle transition range of granular snow ice at the test temperature is 6.67×10^{-5} s^{-1} to 3.11×10^{-4} s^{-1}. The maximum ultimate flexural strength and the corresponding strain rate at each test temperature are summarized in Table 1, which shows that the strain rate corresponding to the maximum ultimate flexural strength value tends to decrease as the temperature decreases. For example, at $-5\,°C$, $-8\,°C$, and $-10\,°C$, the maximum ultimate flexural strengths are 3.19 MPa, 3.29 MPa, and 3.41 MPa, with corresponding strain rates of 3.11×10^{-4} s^{-1}, 1.51×10^{-4} s^{-1}, and 9.78×10^{-5} s^{-1}, respectively, showing a clear reduction with decreasing temperature.

Table 1. Maximum ultimate flexural strength and corresponding strain rate of granular snow ice at different temperatures.

Temperature (°C)	Maximum Ultimate Flexural Strength (MPa)	Strain Rate (s^{-1})
−5	3.19	3.11×10^{-4}
−8	3.29	1.51×10^{-4}
−10	3.41	9.78×10^{-5}
−15	3.45	8.44×10^{-5}
−18	3.48	7.78×10^{-5}
−20	3.50	7.89×10^{-5}
−25	3.53	8.22×10^{-5}
−30	3.56	6.67×10^{-5}
−35	3.57	7.50×10^{-5}

### 3.2.4. The Relationship Between Flexural Strength and Ice Structure

In this study, three-point bending tests on columnar ice were conducted at −20 °C, with loading rates ranging from 0.1 mm/min to 30 mm/min. Figure 7 shows the variation in the flexural strength of columnar ice with strain rate at −20 °C. It reveals that the flexural strength of columnar ice first increases and then decreases with strain rate, but it is lower than that of granular snow ice. The average flexural strength of columnar ice at this temperature is 1.93 MPa, compared to 2.85 MPa for granular snow ice. This is consistent with the results of Timco et al. [37], and Blanchet et al. [55] attributed this phenomenon to the fact that granular ice has a smaller grain size than columnar ice. Cole et al. [56] concluded that stress of ice decreases with increasing grain size. For the same material, a smaller grain diameter results in larger grain boundaries, greater barriers to dislocation motion, higher resistance to deformation and macroscopic strength.
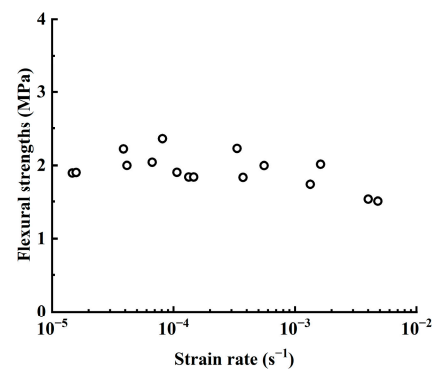
Figure 7. Relationship between flexural strength and strain rate of columnar ice at −20 °C.

Wang [38] conducted three-point bending tests on ice and obtained a fitting equation between flexural strength and temperature. By substituting it, the bending strength at −20 °C was found to be 1.91 MPa. In contrast, this study measures the flexural strength of columnar ice under the same conditions to be 1.70 MPa.

3.2.5. Flexural Failure Mode

Ice cracks can be roughly categorized into two types: one is straight cracks (Figure 8a), where, starting at the lower surface of the ice beam, because of the tension effect of cracks, with the increase in load, the cracks continue to develop upward until they exist throughout the entire specimen, and the destruction of the cross-section is relatively flat. These are type-I tension cracks. The second type is the oblique crack (Figure 8b), where the ice beam is mainly subjected to shear force, and the crack and the direction of tensile stress presents an angle of 30°~45°. This is a type-II shear crack [38].

(**a**) Straight crack   (**b**) Oblique crack
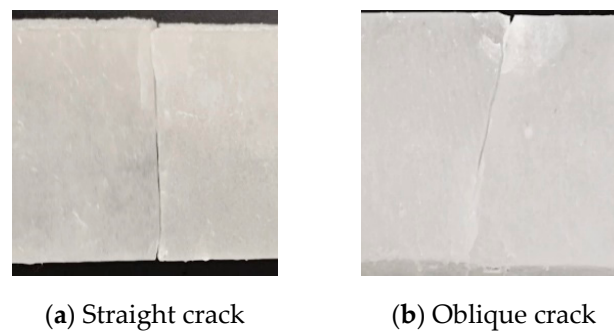
Figure 8. The forms of ice failure under different conditions.

3.3. Fracture Toughness Test

3.3.1. Fracture Process Curve

The fracture toughness was calculated using Formulas (4) and (5), obtaining the fracture toughness values of ice beams at different temperatures and strain rates. A typical granular snow ice-fracture curve is shown in Figure 9. The ice specimen exhibits brittle failure, and after the load reaches its peak, the test shows direct fracturing, with a decrease in bearing capacity to zero. The temperature of the ice specimen is −6 °C, and the loading rate is 0.1 mm/min.
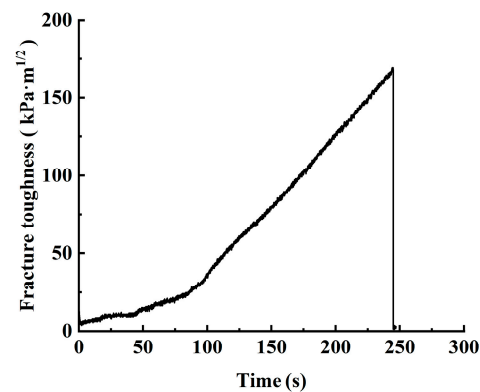
Figure 9. Time variation curve of load at −6 °C and loading rate of 0.1 mm/min.

3.3.2. The Relationship Between Fracture Toughness and Strain Rate

The relationship between ice mechanical properties and loading rate has always been a research focus of engineering ice. Fracture toughness decreases with increasing strain rate due to stress relaxation at the crack tip and material creep [33]. Figure 10 shows the fracture toughness versus strain rate for granular snow ice in the temperature range of −15 °C to −6 °C. At all four temperatures, the fracture toughness tends to decrease with increasing strain rate.

Observation of Figure 10 shows that the fracture toughness has a relatively obvious linear relationship with multiples of strain rate. According to Huang's research [53], this article performs logarithmic fitting on strain rate and fracture toughness:

$$K_{\mathrm{IC}} = A \ln\left(\dot{\varepsilon}/\dot{\varepsilon_0}\right) + B \tag{7}$$

In the formula, K_{IC} represents the fracture toughness of granular snow ice, while A and B are parameters that are temperature-dependent parameters.

As shown in Figure 11, at −10 °C, the fracture toughness peaks at 269.93 kPa·m$^{1/2}$ when the strain rate is 8.0×10^{-6} s^{-1}, and decreases to 98.99 kPa·m$^{1/2}$ when the strain rate increases to 1.53×10^{-3} s^{-1}, representing a 63.33% decrease in fracture toughness.
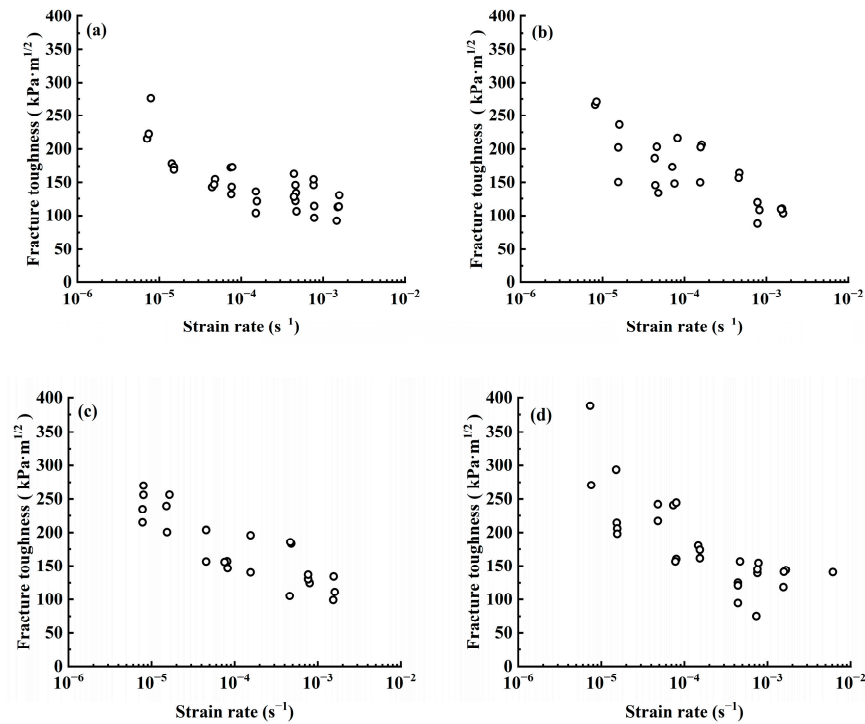
Figure 10. (**a**–**d**) is the relationship between fracture toughness and strain rate (10^{-6} s^{-1}~10^{-2} s^{-1}) of granular snow ice at -6 °C, -8 °C, -10 °C, -15 °C, respectively.
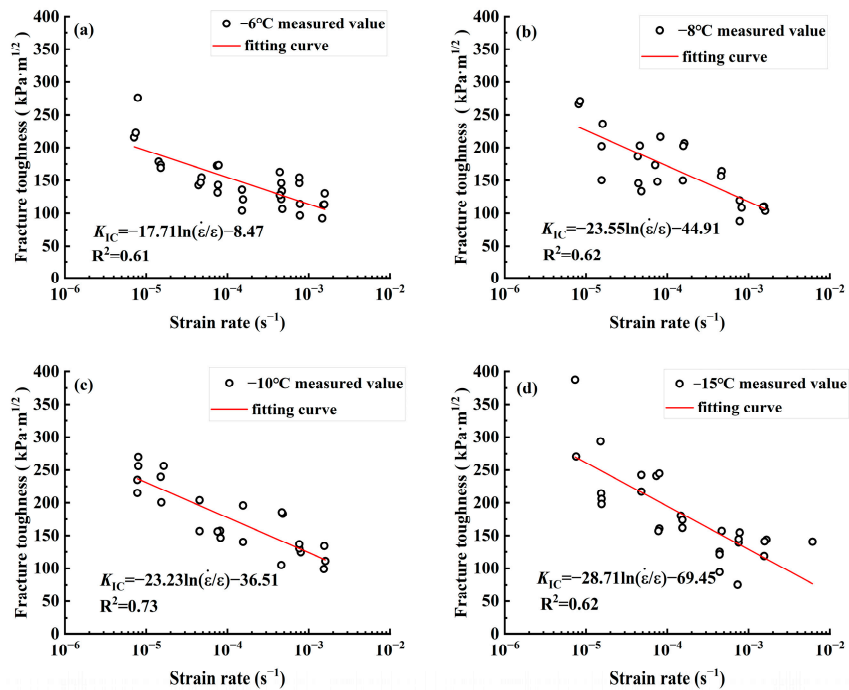
Figure 11. (**a**–**d**) Fit the fracture toughness and strain rate of granular snow ice at -6 °C, -8 °C, -10 °C, and -15 °C, respectively.

Xu et al. [43] conducted three-point bending tests on pure polycrystalline ice with notch at under high loading rates (1 mm/min to 100 mm/min) from -40 °C to -20 °C. They concluded that the fracture toughness of pure polycrystalline ice decreases with increasing strain rate, showing a strong power law relationship between the two. Ji et al. [40] studied the fracture toughness of sea ice and found that the loading rate significantly affects fracture toughness, with the K_{IC} value increasing as the loading rate decreases.

3.3.3. The Relationship Between Fracture Toughness and Temperature

Temperature affects the fracture toughness of ice. By analyzing and organizing data from the three-point flexural fracture test on granular snow ice, changes in fracture toughness at various temperatures were plotted. The average fracture toughness values were 181.60 kPa·m$^{1/2}$, 175.53 kPa·m$^{1/2}$, 167.50 kPa·m$^{1/2}$, and 147.28 kPa·m$^{1/2}$ at temperatures of $-15\,°C$, $-10\,°C$, $-8\,°C$, and $-6\,°C$, respectively. It can be observed that fracture toughness does not differ significantly from $-15\,°C$ to $-8\,°C$ but decreases at $-6\,°C$.

Ji et al. [40] conducted fracture tests on sea ice in the Bohai Sea at temperatures ranging from $-18\,°C$ to $-3\,°C$ and analyzed the relationship between sea ice temperature and fracture toughness. Liu et al. [35] studied artificial columnar ice and found that fracture toughness decreased with increasing temperature in the range of $-30\,°C$ to $-1\,°C$ under a loading rate of 10 mm·s^{-1}. Table 2 presents the average fracture toughness values for the three tests at different temperatures. The fracture toughness values obtained by Liu et al. [35] are slightly lower than those reported in this study due to the lower loading rate. In contrast, the results of Ji et al. [40] are more consistent with the present study. For example, the average fracture toughness in this study at $-10\,°C$ is 175.53 kPa·m$^{1/2}$, compared to 169.0 kPa·m$^{1/2}$ reported by Ji et al. [40]. Although the test conditions resulted in differing fracture toughness values, all three tests concluded that the higher the temperature, the lower the fracture toughness.

Table 2. Average values of fracture toughness in different temperature ranges.
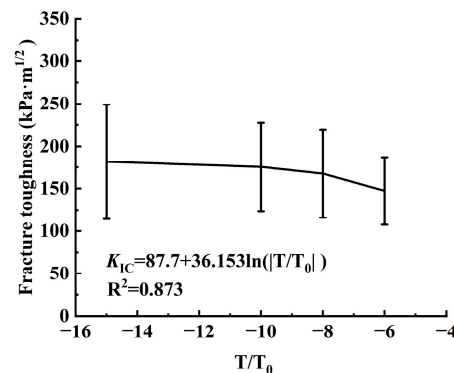
Temperatures (°C)	Ji [40] Fracture Toughness (kPa·m$^{1/2}$)	Liu [35] Fracture Toughness (kPa·m$^{1/2}$)	Fracture Toughness of This Test (kPa·m$^{1/2}$)
-6	131.94	109.74	147.28
-10	169.00	115.18	175.53
-15	215.31	121.97	181.60

Fracture toughness approaches 0 kPa·m$^{1/2}$ as temperature approaches 0 °C. According to Huang's research [53], logarithmic fitting was performed on the relationship between statistical data and fracture toughness with temperature:

$$K_{IC} = C + D\ln(|T/T_0|) \tag{8}$$

In the formula, to coordinate units, adjust the independent variable to T/T_0, where T_0 is a temperature of 1 °C, and C and D are parameters that are temperature-dependent.

Fit the average fracture toughness to the ice temperature. Figure 12 shows the fitting relationship between fracture toughness values and average values of granular snow ice at different temperatures. It is evident that fracture toughness decreases with increasing temperature.

Figure 12. Fitting curves of fracture toughness values and average values of granular snow ice at different temperatures ($-6\,°C$, $-8\,°C$, $-10\,°C$, $-15\,°C$).

3.3.4. Fracture Toughness Failure Mode

In this test, the ice temperature is at −15 to −6 °C, and the displacement loading rate is between 0.05 mm/min and 10 mm/min. In accordance with Formula (3), the strain rate can be calculated. The granular snow ice exhibited brittle failure even at the lowest strain rate. When granular snow ice breaks, a slight sound is produced, and the specimen breaks into two halves. During the test, peeling may sometimes occur near the indenter and at the edge of the granular snow ice. The fracture patterns of the specimens were recorded in this test. Figure 13 shows the fracture morphology of granular snow ice at different temperatures. In the granular snow ice fracture toughness test, 102 ice samples were examined, and we found that 96 samples exhibited straight cracks that progressed upwards from the tip of the prefabricated cracks, with a relatively flat cross-section. Huang [53] conducted three-point flexural fracture tests on Yellow River ice to investigate its fracture failure modes. The results indicated that cracks predominantly developed upward along the tips of pre-existing fractures, and the crack traces were not clearly defined, which aligns with the findings of this study.

(**a**) −6 °C   (**b**) −10 °C   (**c**) −15 °C
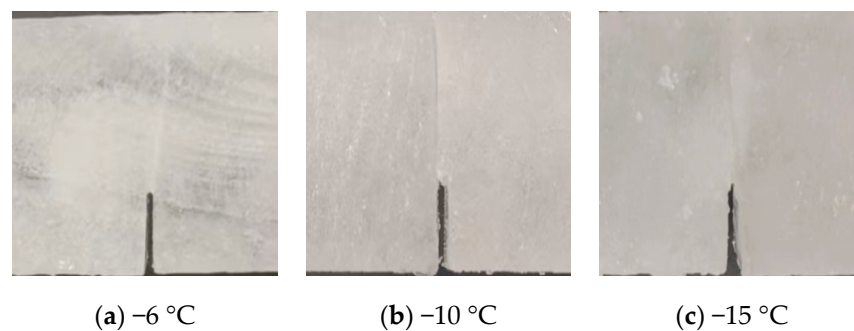
Figure 13. Failure modes of granular snow ice under different temperatures.

4. Conclusions and Future Prospective

To investigate the relationship between bending strength, the fracture toughness of granular ice, temperature, and strain rate, a three-point bending device was employed for both the three-point bending test and the fracture toughness test. Since the fracture toughness cannot be determined directly from the bending test, this study cut prefabricated cracks and then determined the fracture toughness by calculating the critical stress intensity factor. This study supplemented the mechanical properties of granular ice and provided valuable insights for engineering design, construction, and ice sports in cold regions. Specifically, the key findings of this study are as follows:

1. The flexural strength of granular snow ice is influenced by the strain rate and temperature. The bending performance of ice is affected by the strain rate; within the temperature range of −35 to −5 °C, the flexural strength exhibits a trend of first increasing and then decreasing with increasing strain rate. Ice exhibits ductility at low strain rates and brittleness at high strain rates. There exists a ductile–brittle transition interval for ice, ranging from 6.67×10^{-5} s^{-1} to 3.11×10^{-4} s^{-1}. The lower the temperature, the higher the flexural strength of ice, but the more pronounced its brittle characteristics, manifesting as a lower strain rate corresponding to the maximum flexural strength. For example, at −5 °C, the strain rate corresponding to the maximum flexural value is 3.11×10^{-4} s^{-1}, while at −10 °C, the strain rate corresponding to the maximum flexural strength is only 6.67×10^{-5} s^{-1}. The flexural strength is influenced by the crystal structure: at −20 °C, the average flexural strength of granular snow ice is 2.85 MPa, while under the same temperature, the average flexural strength of columnar ice is 1.93 MPa.

2. The fracture toughness of granular snow ice is influenced by strain rate and temperature. Within the range of −15 to −6 °C, fracture toughness decreases as the strain rate increases. Temperature similarly affects fracture toughness, with higher temperatures

resulting in lower values. At $-15\,°C$, the fracture toughness is 181.60 kPa·m$^{1/2}$, but it decreases to 147.28 kPa·m$^{1/2}$ at $-6\,°C$.

3. In the three-point bending test, the crystal structure, temperature, and strain rate of ice do not significantly influence the fracture mode. Ice cracks can be categorized into two types: straight cracks that develop along grain boundaries and oblique cracks that form at a specific angle to the direction of tensile stress. In the three-point bending test of granular snow ice with a notch, 102 ice samples were analyzed, 96 of which exhibited vertical fractures.

In addition, there are still some limitations in this study that need to be addressed and explored in future research:

1. In practical applications, the temperature of the ice layer varies with depth. The experiment controls the sample temperature to be uniform, but the influence of temperature non-uniformity on ice mechanics parameters has not been explored. In subsequent research, theory should be combined with practice, and the bending strength and fracture toughness obtained from experiments should be used to provide support for the design and construction of ice sports projects and cold-region engineering.

2. In the fracture toughness test, we only analyzed the fracture toughness of granular ice at $-15\,°C$ to $-6\,°C$. In the future, fracture toughness tests can be conducted on granular ice at different temperatures, and better analytical methods can be found to analyze its fracture toughness.

References

1. Mironov, E.U.; Egorova, E.S. Seasonal and interannual variations in the Greenland Sea ice age composition in the winter period. *Russ. Meteorol. Hydrol.* **2024**, *49*, 221–229. [CrossRef]
2. Zhang, Y.X.; Qiu, Y.B.; Li, Y.; Leppäranta, M.; Jia, G.; Jiang, Z.X.; Liang, W.S. Spatial-temporal variation of river ice coverage in the Yenisei river from 2002 to 2021. *J. Hydrol.* **2024**, *637*, 131440. [CrossRef]
3. Zhang, L. A Study on the Brazilian Disk Splitting Test of Antarctic Ice and Liaohe Ice. Master's Thesis, Dalian University of Technology, Dalian, China, 2022. (In Chinese)
4. Zhang, Y. Study on the Internal Structure and Surface Crack Characteristics of River Ice. Master's Thesis, Shenyang Agricultural University, Shenyang, China, 2019. (In Chinese)
5. Makkonen, L.; Tikanmäki, M.; Sainio, P. Friction in sliding heavy objects on ice. *J. Glaciol.* **2016**, *62*, 1186. [CrossRef]
6. Cheng, P.; Li, J.; Li, X. Analysis of carrying capacity of ice cover based on Winkler Model. *Yangtze River* **2017**, *48*, 64–68. (In Chinese) [CrossRef]
7. Yan, Y.; Zhang, J.; Wang, Y.; Tao, Y.; Xu, Y.; Gu, W. Spatiotemporal distribution characteristics of sea ice disasters in the Northern China Sea from 2001 to 2020. *Ocean Coast. Manag.* **2023**, *246*, 106889. [CrossRef]
8. Xiu, Y.R.; Li, Z.J.; Wang, Q.K.; Han, H.W. Experimental study on the bending mechanical behavior of granular sea ice in Liaodong Bay. *Mar. Sci. Bull.* **2023**, *42*, 667–676. (In Chinese)
9. Zhang, Y.; Qian, Z.; Lv, S.; Huang, W.; Ren, J.; Fang, Z.; Chen, X. Experimental investigation of uniaxial compressive strength of distilled water ice at different growth temperatures. *Water* **2022**, *14*, 4079. [CrossRef]
10. Long, X.; Liu, S.; Ji, S. Discrete element modelling of relationship between ice breaking length and ice load on conical structure. *Ocean Eng.* **2020**, *201*, 107152. [CrossRef]
11. Yu, J. Experimental Study on Physical and Mechanical Properties of Artificially Frozen Ice Considering Irradiation Effects. Master's Thesis, Northeast Agricultural University, Harbin, China, 2021. (In Chinese)

12. Zhang, H.B. Experimental Study on Tensile Strength and Fracture Toughness of Yellow River Ice by Using Split Test. Master's Thesis, Dalian University of Technology, Dalian, China, 2016. (In Chinese)
13. Zhang, X.P.; Chen, K.; Li, F.; Xing, H.N. Experimental study of the fracture toughness of natural freshwater ice. *J. Glaciol. Geocryol.* **2010**, *32*, 960–963. (In Chinese)
14. Weeks, W.F.; Assur, A. The mechanical properties of sea ice. In *US Army Cold Regions Research and Engineering Laboratory (CRREL) Monograph II-C3*; Cold Regions Research and Engineering Laboratory: Hanover, NH, USA, 1967.
15. Sinha, N.K. Short-term rheology of polycrystalline ice. *J. Glaciol.* **1978**, *21*, 457–474. [CrossRef]
16. Lee, R.W.; Schulson, E.M. The strength and ductility of ice under tension. *J. Offshore Mech. Arct. Eng.* **1988**, *110*, 187–191. [CrossRef]
17. Schulson, E.M.; Renshaw, C.E. Fracture, friction, and permeability of ice. *Annu. Rev. Earth Planet. Sci.* **2022**, *50*, 323–343. [CrossRef]
18. Wang, C.; Han, D.; Wang, Q.; Wang, Y.; Zhang, Y.; Jing, C. Study of elastoplastic deformation and crack evolution mechanism of single-crystal ice during uniaxial compression using 3D digital image correlation. *Eng. Fract. Mech.* **2023**, *293*, 109712. [CrossRef]
19. Chen, X.D.; Wang, A.L.; Ji, S.Y. The study on brittle-ductile transition mechanism and failure mode of sea ice under uniaxial compression. *Sci. Sin.-Phys. Mech. Astron.* **2018**, *48*, 124601. [CrossRef]
20. Zhang, Y.; Li, Z.; Guo, W.; Yu, H.; Liang, W. Method and equipment for three-pint flexural strength test of ice. *Hydro Sci. Cold Zone Eng.* **2018**, *1*, 63–68. (In Chinese)
21. Schulson, E.M. Brittle failure of ice. *Eng. Fract. Mech.* **2001**, *68*, 1839–1887. [CrossRef]
22. Schulson, E.M. An analysis of the brittle to ductile transition in polycrystalline ice under tension. *Cold Reg. Sci. Technol.* **1979**, *1*, 87–91. [CrossRef]
23. Yasui, M.; Schulson, E.M.; Renshaw, C.E. Experimental studies on mechanical properties and ductile-to-brittle transition of ice-silica mixtures: Young's modulus, compressive strength, and fracture toughness. *J. Geophys. Res. Solid Earth* **2017**, *122*, 6014–6030. [CrossRef]
24. Kellner, L.; Stender, M.; Herrnring, H.; Ehlers, S.; Hoffmann, N.; Høyland, K.V. Establishing a common database of ice experiments and using machine learning to understand and predict ice behavior. *Cold Reg. Sci. Technol.* **2019**, *162*, 56–73. [CrossRef]
25. Meng, D.; Chen, X.; Ji, S. Experimental study on the flexural strength and failure process of sea ice. *Mar. Sci. Bull.* **2021**, *40*, 609–620. (In Chinese) [CrossRef]
26. Zhang, J.; Mou, J.; Pan, Z.; Li, Y. Discussion and prospects of the development on measurement while drilling technology in oil and gas wells. *Petrol. Sci. Bull.* **2024**, *9*, 240–259. (In Chinese) [CrossRef]
27. Efimov, V.P. Experimental study on loading rate effects on the tensile strength and fracture toughness of rocks. *Geotech. Geol. Eng.* **2020**, *38*, 1–8. [CrossRef]
28. Yin, T.; Wu, Y.; Wang, C.; Zhuang, D.; Wu, B. Mixed-mode I+II tensile fracture analysis of thermally treated granite using straight-through notch Brazilian disc specimens. *Eng. Fract. Mech.* **2020**, *234*, 107111. [CrossRef]
29. Abdolghanizadeh, K.; Hosseini, M.; Saghafiyazdi, M. Effect of freezing temperature and number of freeze–thaw cycles on mode I and mode II fracture toughness of sandstone. *Theor. Appl. Fract. Mech.* **2020**, *105*, 102428. [CrossRef]
30. Xu, Y.; Yao, W.; Zhao, G.; Xia, K. Evaluation of the short core in compression (SCC) method for measuring mode II fracture toughness of rocks. *Eng. Fract. Mech.* **2020**, *224*, 106747. [CrossRef]
31. Xiao, Z. Reliability Study on the Brazilian Test Method for Determining the Mechanical Properties of Ice. Master's Thesis, Dalian University of Technology, Dalian, China, 2017. (In Chinese).
32. Han, H.W.; Jia, Q.; Huang, W.F.; Li, Z.J. Flexural strength and effective modulus of large columnar-grained freshwater ice. J. *Cold Reg. Eng.* **2016**, *30*, 04015005. [CrossRef]
33. Timco, G.W. Flexural strength and fracture toughness of urea model ice. *J. Energy Resour. Technol.* **1985**, *107*, 498–505. [CrossRef]
34. Petrovic, J.J. Review mechanical properties of ice and snow. *J. Mater. Sci.* **2003**, *38*, 1–6. [CrossRef]
35. Liu, H.W.; Miller, K.J. Fracture toughness of fresh-water ice. *J. Glaciol.* **1979**, *22*, 135–143. [CrossRef]
36. Nixon, W.A.; Schulson, E.M. The fracture toughness of ice over a range of grain sizes. *J. Offshore Mech. Arct. Eng.* **1988**, *110*, 192–196. [CrossRef]
37. Timco, G.W.; Frederking, R.M.W. Flexural strength and fracture toughness of sea ice. *Cold Reg. Sci. Technol.* **1983**, *8*, 35–41. [CrossRef]
38. Wang, L. Experimental Study on the Bending Resistance of Artificial Ice and Numerical Simulation Analysis of Artificial Ice Rinks. Master's Thesis, Harbin Institute of Technology, Harbin, China, 2021. (In Chinese).
39. Gagnon, R.E.; Gammon, P.H. Characterization and flexural strength of iceberg and glacier ice. *J. Glaciol.* **1995**, *41*, 103–111. [CrossRef]
40. Ji, S.; Liu, H.; Xu, N.; Ma, H. Experiments on sea ice fracture toughness in the Bohai Sea. *Adv. Water Sci.* **2013**, *24*, 386–391. (In Chinese) [CrossRef]
41. Zhang, A.D.; Ji, H.L.; Li, Z.J.; Zhang, B.S.; Xu, J. Experimental research on flexural strength of fresh water ice in Hongqipao Reservoir in Da-qing. *Chin. Rural Water Hydropower* **2011**, *3*, 70–72. (In Chinese)
42. Zhang, L.Z. Flexural strength and effective modules of Songhua River ice. *Adv. Mater. Res.* **2013**, *2569*, 783–793. [CrossRef]
43. Xu, X.; Jeronimidis, G.; Atkins, A.G.; Trusty, P.A. Rate-dependent fracture toughness of pure polycrystalline ice. *J. Mater. Sci.* **2004**, *39*, 225–233. [CrossRef]

44. Litwin, K.L.; Zygielbaum, B.R.; Polito, P.J.; Sklar, L.S.; Collins, G.C. Influence of temperature, composition, and grain size on the tensile failure of water ice: Implications for erosion on Titan. *J. Geophys. Res.* **2012**, *117*, E08013. [CrossRef]
45. Mulmule, S.V.; Dempsey, J.P. Scale effects on sea ice fracture. *Mech. Cohesive-Frict. Mater.* **1999**, *4*, 505–524. [CrossRef]
46. Dempsey, J.P.; Adamson, R.M.; Mulmule, S.V. Scale effects on the in-situ tensile strength and fracture of ice. Part II: First-year sea ice at Resolute, NWT. *Int. J. Fract.* **1999**, *95*, 347–366. [CrossRef]
47. Yuan, B.J. Research and Application of Artificial Ice Failure Criteria in Ice Rink. Master's Thesis, Harbin Institute of Technology, Harbin, China, 2021. (In Chinese)
48. Huang, W.F.; Li, Z.J.; Han, H.W.; Jia, Q. Seasonal evolution of static freshwater lake ice microstructures and the effects of growth processes. *J. Glaciol. Geocryol.* **2016**, *38*, 699–707. (In Chinese)
49. Schwarz, J.; Frederking, R.; Gavrillo, V.; Petrov, I.G.; Hirayama, K.I.; Mellor, M.; Tryde, P.; Vaudrey, K.D. Standardized testing methods for measuring mechanical properties of ice. *Cold Reg. Sci. Technol.* **1981**, *4*, 245–253. [CrossRef]
50. Han, H.W. Study on the Spatial and Temporal Distribution of Sea Ice and the Physical, Mechanical Properties of Sea Ice in Polar Routes. Doctoral Thesis, Dalian University of Technology, Dalian, China, 2016. (In Chinese)
51. Gold, L.W. Some observations on the dependence of strain on stress for ice. *Can. J. Phys.* **1958**, *36*, 1265–1275. [CrossRef]
52. Wei, J.; Zhu, W.C.; Li, R.F.; Niu, L.L.; Wang, Q.Y. Experiment of the tensile strength and fracture toughness of rock using notched three point bending test. *J. Water Resour. Archit. Eng.* **2016**, *14*, 128–142. (In Chinese)
53. Huang, Y. Experimental Study on the Fracture Performance of the Yellow River Ice During Freezing Period. Master's Thesis, Zhengzhou University, Zhengzhou, China, 2021. (In Chinese)
54. Han, H.W.; Li, Z.J.; Zhang, L.M.; Qing, X.X.; Zhou, Q. Experimental Study on Three Point Bending Mechanical Properties of Sea Ice in Taiping Bay, Bohai Sea. In Proceedings of the National Conference on Hydraulic and Hydraulic Informatics, Tianjin, China, 13 October 2011. (In Chinese)
55. Blanchet, D.; Abdelnour, R.; Comfort, G. Mechanical properties of first-year sea ice at Tarsiut Island. *J. Cold Reg. Eng.* **1997**, *11*, 59–83. [CrossRef]
56. Cole, D.M. The microstructure of ice and its influence on mechanical properties. *Eng. Fract. Mech.* **2001**, *68*, 1797–1822. [CrossRef]